Available online at www.sciencedirect.com

ScienceDirect

IFAC Papers Online CONFERENCE PAPER ARCHIVE

IFAC-PapersOnLine 49-11 (2016) 461–468

# Simultaneous Estimation of Intake and Residual Mass Using In-Cylinder Pressure in an Engine with Negative Valve Overlap

**C. Guardiola** * **V. Triantopoulos** ** **P. Bares** * **S. Bohac** ** **A. Stefanopoulou** **

* *CMT–Motores Térmicos, Universitat Politècnica de València, Valencia, Spain (e-mail:* {carguaga,pabamo}*@mot.upv.es).*
** *Department of Mechanical Engineering, University of Michigan, Ann Arbor, Michigan, USA (e-mail:* {vtrianto,sbohac,annastef}*@umich.edu)*

**Abstract:**
This work presents a new method for the simultaneous estimation of the intake and residual mass in an engine operating with negative valve overlap. The method exclusively uses the in-cylinder pressure information and no additional measurement is needed. It is based on the determination of the total mass through the pressure resonance in the cylinder and the assumption of a polytropic expansion of the gas during the exhaust stroke for determining the residual gases. The method has been demonstrated on an engine with negative valve overlap operating in SI, SACI and HCCI combustion. The results show that the proposed method can provide good mass estimations in most cycles in HCCI and SACI combustion, and in lightly knocking cycles while operating in SI combustion.



*Keywords:* In-cylinder pressure, residual mass, air mass, estimation, negative valve overlap, HCCI, SACI, SI

## 1. INTRODUCTION

Cylinder charge determination in internal combustion engines is a difficult task, which is usually achieved through the combination of different measurement and modelling techniques for the individual determination of the external flows (air, fuel, recirculated gas) and the residual gases. Most of the standard techniques rely on sensors that are slower than the characteristic engine cycle time, and then cannot provide a proper description in the case of fast transients or significant cycle-to-cycle variability, as is a common situation in low temperature combustion (LTC) modes.

LTC modes, such as homogeneous charge compression ignition (HCCI) and spark assisted compression ignition (SACI) combustion, have shown potential in increasing the thermal efficiency of the conventional spark ignited (SI) engine, while maintaining low or easily treatable engine-out emissions (Zhao et al., 2002; Manofsky et al., 2011). For the practical implementation of these LTC modes, an exhaust gas recompression strategy is often employed using negative valve overlap (NVO), as this strategy provides fast control of the gas charge composition and temperature, which directly impacts combustion phasing (Cairns and Blaxill, 2005; Wheeler et al., 2013). In NVO engines, the exhaust valve closes well before top dead center of the exhaust stroke, as shown in Figure 1, thereby trapping high levels of residual exhaust gas necessary to promote autoignition of the charge in the following cycle. However, the temperature and composition of the charge have to be well controlled to achieve the appropriate top dead center

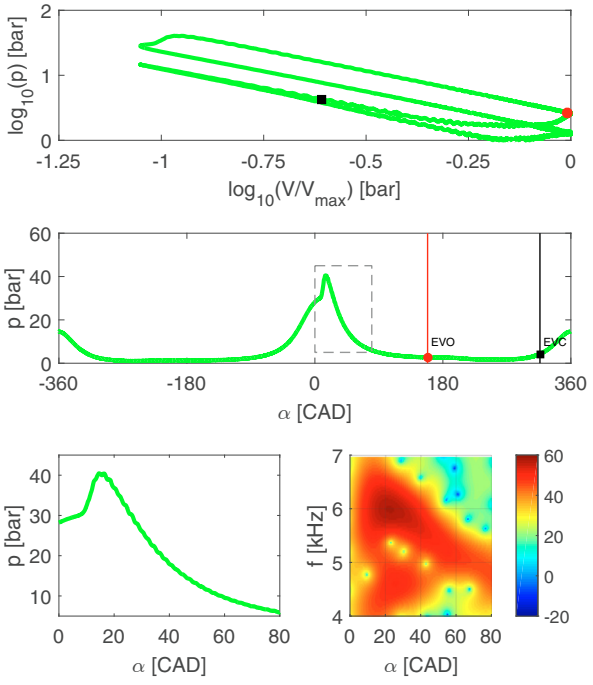


Fig. 1. Unfiltered pressure trace of a given cycle operating with NVO; EVO and EVC have been marked. Left bottom plot is a zoom of the 0 to 80 CAD region showing pressure resonance phenomenon. Right plot is the spectrogram of that section in the region from 4 to 7 kHz; power spectral density is expressed in logarithmic scale (dB/rad/sample).


Peer review under responsibility of International Federation of Automatic Control.
10.1016/j.ifacol.2016.08.068

(TDC) conditions for optimal combustion characteristics (Lavoie et al., 2010).

For the case of an HCCI engine with NVO, Hellström et al. (2013) developed a two-state deterministic model able to predict the mean combustion phasing behavior via the evolution of recycled thermal and chemical energy carried from cycle-to-cycle through the trapped residuals. The global characteristics of the cyclic variability at various operating points were also captured in Hellström et al. (2013) by introducing a small random perturbation on top of the predicted mean residual mass. The prediction of the cyclic dispersion patterns led to cycle-to-cycle control of fuel injection for reducing the combustion variability (Hellström et al., 2014). Analysis of various model-based control techniques in Hellström et al. (2014) showed high sensitivity away from the nominal operating conditions, hence an improved calculation of the residual mass could augment the modeled residuals and improve the control robustness.

A number of residual estimation methods based on in-cylinder pressure information for engines operating with NVO are available in the literature, as summarized and compared by Ortiz-Soto et al. (2012):

- State Equation method, where the exhaust temperature is propagated from the exhaust manifold to the cylinder and the residual mass is calculated through the application of the state equation at the exhaust valve closing (EVC):

$$m_{res} = \frac{p_{EVC} V_{EVC}}{R T_{exh}} \tag{1}$$

- Yun and Mirsky (1974) method, where the gas mixture is assumed to evolve according to a polytropic and the measured intake mass flow is compared with the state equation evaluated at both exhaust valve opening (EVO) and EVC:

$$m_{res} = \frac{(m_a + m_f + m_{egr}) \frac{V_{EVC}}{V_{EVO}} \left(\frac{p_{EVC}}{p_{EVO}}\right)^{\frac{1}{\gamma}}}{1 - \frac{V_{EVC}}{V_{EVO}} \left(\frac{p_{EVC}}{p_{EVO}}\right)^{\frac{1}{\gamma}}} \tag{2}$$

- Fitzgerald method (Fitzgerald et al., 2010), which also uses the measured intake mass flow for solving the mass difference between EVO and EVC, but the in-cylinder temperature evolution during the exhaust stroke is modeled combining the convective heat transfer equation with the assumption of $T_{exh}$ to be representative of the mean temperature inside the cylinder. Woschni correlation (Woschni, 1967) is used for the heat transfer coefficients.

Despite the fact that in-cylinder pressure measurement is fast enough to provide cycle-to-cycle information, in all methods presented above in-cylinder pressure information is combined with another variable to estimate residual mass. Exhaust temperature, $T_{exh}$, is used as an approximation of in-cylinder temperature during the exhaust process in the State Equation and Fitzgerald methods, and intake mass flow in the Yun and Mirsky and Fitzgerald methods. However, such assumptions present significant drawbacks with the most important being the difficulty to properly represent transient or cycle-to-cycle variability since the method is hampered by the slow response of both exhaust temperature and mass flow sensors. Even if fast sensors are available in a laboratory setting, their time constants for a durable on-board application is not sufficient to provide cycle-to-cycle information, hence the existing method assumptions are not fulfilled.

Residual estimation in an HCCI engine operating with significant cyclic variability has been addressed by several authors. Larimore et al. (2013) developed an online estimator of the residual gas fraction, where blowdown temperature is modeled in order to consider the effect of the residual temperature on the next cycle. In Larimore et al. (2015) a real time implementation of Fitzgerald's method was presented and the effect of errors in the determination of $T_{exh}$ was analyzed, concluding that there is a low sensitivity of the residual mass estimation to errors in $T_{exh}$. Once again, and as pointed out by the authors, the main limitation of the algorithm is that it requires a transient air mass as an input.

With the aim of overcoming these difficulties, this paper presents a new method which exclusively relies on the in-cylinder pressure signal for simultaneously providing an estimation of the mass flow entering the cylinder and the residual gas mass. The method takes benefit of the excitation of resonant modes in the cylinder by the combustion, which produces pressure oscillations following the combustion as depicted in the lower left plot in Figure 1, for deriving the mix temperature during the expansion stroke and determining the total cylinder mass (Guardiola et al., 2014). This total mass estimate is then combined with the assumption of an adiabatic expansion during the exhaust phase, as in Yun and Mirsky method, for discerning between external and residual mass for the case of NVO engines. Since only pressure information is used and no temperature or flow measurement is needed, the method is expected to have a better time response than the existent methods in the literature.

## 2. EXPERIMENTAL SETUP

In this study, experiments were performed on a modified 2010 GM LNF Ecotec I4 spark-ignited engine. The engine has been modified to enable multi-mode combustion, including conventional SI, SACI and HCCI combustion. The compression ratio of the engine has been increased from 9.2:1 to 11.25:1, with custom pistons and head machining. The main characteristics of the engine are shown in Table 1.

| | |
|---|---|
| Number of cylinders | 4 |
| Bore (B) | 86 mm |
| Stroke (S) | 86 mm |
| Conrod length (L) | 145.5 mm |
| Compression ratio (cr) | 11.25 |

Table 1. Engine main characteristics.

The engine is equipped with DOHC, dual variable valve timing (VVT) with 50 degrees of crank angle degree phasing authority. A negative valve overlap camshaft set was used in this work with maximum lift of 3.5 mm and 154 crank angle degrees duration, defined at 0 mm opening. A high-pressure cooled EGR system has been added to the engine with associated flow control, which is connected downstream of a 58 mm throttle body. The throttle and

EGR entry location have been moved further upstream in the air path to allow for better EGR mixing. An Eaton R-410 supercharger has been added to the air path to provide intake boost, along with the stock twin scroll, waste-gated Model K04 BorgWarner turbocharger. A back pressure valve has been installed downstream of the turbocharger to better control the external EGR rate. The fuel used is UTG-96 Federal Certification Gasoline with a RON = 96.0 and MON = 88.6.

Cylinder pressure from all 4 cylinders was sampled at 0.1 crank angle degrees using Kistler 6125A piezoelectric pressure transducers. Cylinder 1 was additionally instrumented with Kistler piezoresistive absolute pressure sensors near the exhaust and intake ports, the latter used for cylinder pressure pegging. The analysis presented in this work uses cylinder pressure data from cylinder 1.

Fuel mass $m_f$ was measured using a Pierburg PLU 103 positive displacement volumetric flowmeter. Fresh air mass $m_a$ in steady operation was determined from $m_f$ and equivalence ratio provided by a Horiba MEXA 7500 DEGR exhaust analyzer, sampling from exhaust runner of cylinder 1. For the tests running with external EGR, intake $CO_2$ concentration was measured from the intake manifold and used, together with $m_a$ and exhaust $CO_2$ concentration, to determine the EGR mass $m_{egr}$.

According to the definitions used in the present work, total mass inside the cylinder would be:

$$m_{cyl} = m_a + m_f + m_{egr} + m_{res} \tag{3}$$

where $m_{res}$ is the residual mass to be determined. The exhaust mass leaving the cylinder for a given cycle $k$ would be:

$$m_{exh}(k) = m_{cyl}(k) - m_{res}(k) \tag{4}$$

considering $m_{res}(k)$ the residuals from cycle $k$ to cycle $k+1$. Note that the expected average value for $m_{exh}$ is the measured $m_a + m_f + m_{egr}$.

## 3. METHOD DESCRIPTION

The proposed method is based on the determination of the in-cylinder mass and temperature of the mixture during the expansion stroke by taking advantage of the existence of resonant modes in the in-cylinder pressure, which are excited as a result of the combustion event. The lower left plot in Figure 1 shows a zoom of the 20 to 80 CAD segment of the in-cylinder pressure trace, while the lower right plot shows a spectrogram for this section and the frequency range from 4 to 7 kHz. It can be clearly seen that the frequency varies as the expansion stroke takes place.

As shown in Draper (1935), resonance frequency depends on cylinder geometry and the speed of sound, following:

$$f_{cyl} = \frac{aB}{\pi D} \tag{5}$$

where $f_{cyl}$ is the resonance frequency, $B$ is the Bessel coefficient for the first radial mode, $D$ is the cylinder bore, and $a = \sqrt{\gamma RT} = \sqrt{\gamma pV/m}$ is the speed of sound.

The variation of $f_{cyl}$ along the expansion stroke shown in the spectrogram in Figure 1 is a consequence, on one hand, of the decrease of the gas temperature and, on the other hand, of the modification of the Bessel coefficient, $B$. $B$ remains constant only when the radial section does not change, which is not true in most internal combustion engines. When a combustion chamber with a bowl is considered, $B$ varies with the engine angular position ($\alpha$). Nevertheless, $B(\alpha)$ results in an engine characteristic and stands invariable for a given engine for every operation condition.

The first application of (5) to estimate in-cylinder conditions was done by Hickling et al. (1983) for temperature estimation in internal combustion engines, while the approach was later systematized by Guardiola et al. (2014) for inferring the trapped mass. The core of the latter method is determining $f_{cyl}(\alpha)$ through the short time Fourier transform (STFT) applied over a crank angle window after the end of the combustion, once the in-cylinder temperature may be considered homogeneous (Broatch et al., 2015a). The trapped mass is then determined by:

$$\hat{m}_{cyl}(\alpha) = \left( \frac{B(\alpha)\sqrt{\gamma p(\alpha) V(\alpha)}}{\pi D f_{cyl}(\alpha)} \right)^2 \tag{6}$$

where $p$ is the in-cylinder pressure, $V$ the cylinder volume and $\gamma$ the specific heat ratio of the mix. In this expression, a zero-phase low pass filter with cut-off frequency below the resonance frequency range (e.g. 2 kHz) is applied to the in-cylinder pressure in order to avoid the propagation of its oscillations to the mass estimation.

Note that (6) provides an estimate of the mass for each position of the crankshaft, so it is possible to derive error metrics for a given cycle:

$$\begin{aligned} m_{cyl} &= median\left(\hat{m}_{cyl}(\alpha)\right) \\ \sigma_{m_{cyl}} &= std\left(\hat{m}_{cyl}(\alpha)\right) \end{aligned} \tag{7}$$

For the present application, median value has been preferred over mean value for the final implementation due its higher robustness for outlier rejection. An alternative formulation in Broatch et al. (2015b) compacts the time-frequency analysis, (6) and (7) in a direct transform that provides cylinder mass from pressure.

Once total mass $m_{cyl}$ has been determined, it is possible to derive the cylinder conditions at EVO:

$$T_{EVO} = \frac{p_{EVO} V_{EVO}}{m_{cyl} R} \tag{8}$$

This estimate of the temperature at exhaust valve opening replaces the need to use the exhaust temperature measurement, as in the State Equation method. The exhaust process is then modeled as an isentropic process and the residual mass (i.e. cylinder mass at EVC) may be calculated:

$$m_{res} = \frac{p_{EVC} V_{EVC}}{T_{EVC} R} = \frac{p_{EVC} V_{EVC}}{T_{EVO} \left(\frac{p_{EVC}}{p_{EVO}}\right)^{\frac{\gamma-1}{\gamma}} R} \tag{9}$$

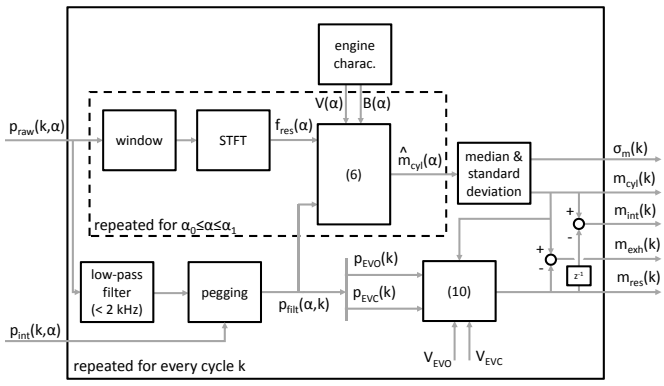


ig. 2. Method block diagram.

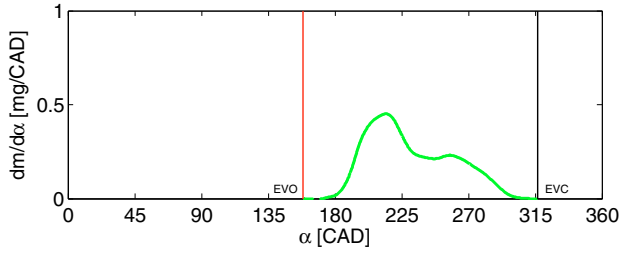


ig. 3. Calculated exhaust mass flow for a given engine cycle.

'ombining these last two expressions:

$$m_{res} = m_{cyl} \frac{V_{EVC}}{V_{EVO}} \left( \frac{p_{EVC}}{p_{EVO}} \right)^{\frac{1}{\gamma}} \tag{10}$$

inally, the intake and exhaust flow during intake and xhaust strokes may be determined by analyzing the ıccession $m_{cyl}$ and $m_{res}$:

$$\begin{aligned} m_{exh}(k) &= m_{cyl}(k) - m_{res}(k) \\ m_{int}(k) &= m_{cyl}(k) - m_{res}(k-1) \end{aligned} \tag{11}$$

'here $k$ refers to the pressure cycle used for computing ıe mass flows.

; is possible to derive the relationship between $m_{cyl}$ and $_{exh}$ by the combination of (10) and (11):

$$m_{cyl} = \frac{m_{exh}}{1 - \frac{V_{EVC}}{V_{EVO}} \left( \frac{p_{EVC}}{p_{EVO}} \right)^{\frac{1}{\gamma}}} \tag{12}$$

'ote the similarity between Yun and Mirsky method (2), nd the combination of (10) and (12). The only difference : that Yun and Mirsky method uses $m_{exh} = m_a + m_f + _{egr}$ for determining $m_{cyl}$ and $m_{res}$, while in the present ıethod the use of the mass flow measurement is avoided s $m_{cyl}$ is derived from the pressure resonance.

igure 2 summarizes in a block diagram the main opera- ons and signal manipulations. As the first mode of the esonance is in the range of 3 to 7 kHz, in-cylinder pressure 'equency contents must be preserved (i.e. non filtered) p to 15 kHz in order to avoid aliasing. This corresponds ɔ a minimum angular resolution of 0.5 CAD/sample at 250 rpm as an indicative value. In addition, if the engine speed is not sufficiently constant during the cycle, time-based acquisition of the pressure signal is advised in order to preserve the accuracy in the determination of $f_{cyl}$.

Furthermore, if (9) is used during the complete evolution of the exhaust stroke, it is possible to infer the exhaust flow through the valve, as depicted in Figure 3.

### *3.1 On gas properties and heat transfer during the exhaust stroke*

In its present formulation the method does not consider the effect of gas mix composition or in-cylinder heat transfer during the exhaust stroke. Both of them could be considered, but at the cost of using an iterative implementation.

It should be noted that if only residual and total masses are to be computed (and not T or instantaneous mass flow), the method only makes use of $\gamma$. In Guardiola et al. (2014) it is quantified that the total error due to the effect of composition on $\gamma$ is lower than 2%. For the present work, $\gamma = 1.3$ has been selected as a characteristic value of the combustion gases.

### *3.2 On method calibration*

One of the difficulties for deploying the method is the determination of the geometry dependent Bessel coefficient $B(\alpha)$ in (6). There are several approaches for finding it:

- Model based approach, as in Broatch et al. (2015a), where the Finite Element Method is used for calculating the resonance frequency of the cylinder at different crankshaft positions.
- Data based approaches: in this case real pressure traces of a single operation point or of a set of operation points are used for determining the angular variation of the Bessel coefficient by inversion of (6):

$$B(\alpha) = \frac{\pi D f_{cyl}(\alpha) \sqrt{m_{cyl}}}{\sqrt{\gamma p(\alpha) V(\alpha)}} \tag{13}$$

  However, determining the actual value of $B$ requires an estimation of a reference $m_{cyl}$ for the calibration dataset. Several options are possible:
  - Using a combination of external measurements for $m_{exh} = m_f + m_a + m_{egr}$ and a residual mass model as, for example, the emptying-and-filling model described in Payri et al. (2007), or other models (e.g. high fidelity one dimensional models) or methods (e.g. the $\Delta p$ method in Desantes et al. (2010)) able to provide an estimation of the total mass inside the cylinder.
  - Deriving the cylinder mass from $m_{exh}$ through (12). In this case the Bessel coefficient is calibrated for matching the exhaust mass $m_{exh}$ rather than the total cylinder mass. Note however that $m_{exh}$ may be externally measured through a combination of state-of-the-art instruments and methodologies ($m_{exh} = m_a + m_f + m_{egr}$), which is not the case for $m_{res}$.
  - Finally, if not sufficient information is available for $m_{cyl}$ or $m_{exh}$, it can be assumed that the cylinder behaves as a cylinder of bore $D$ and infinite length when the piston moves away from

the top dead center. Therefore, B tends towards 1.841 (Draper, 1935; Broatch et al., 2015a) and the reference $m_{cyl}$ can be estimated by:

$$m_{cyl} = \left( \frac{1.841 \sqrt{\gamma p\left(\alpha_\infty\right) V\left(\alpha_\infty\right)}}{\pi D f_{cyl}\left(\alpha_\infty\right)} \right)^2 \qquad (14)$$

where $\alpha_\infty$ is sufficiently far from the top dead center. Once $m_{cyl}$ reference is estimated, the complete function $B\left(\alpha\right)$ can be determined through (13).

It should be noted that, with independence of the calibration method used, $B\left(\alpha\right)$ is a geometric characteristic and stands invariable for any operation condition. As $B\left(\alpha\right)$ only depends on the geometry, it will be the same for any unit of a given engine model.

## 4. RESULTS AND DISCUSSION

The engine was tested in different operating conditions and combustion modes. These included conventional spark ignited (SI), homogeneous charge compression ignition (HCCI) and spark assisted compression ignition (SACI). Figure 4 shows three examples of pressure traces and apparent heat release law (HRL) corresponding to the three different operating modes. Selected examples were run at 2000 rpm, with $\lambda$=0.9793 and IMEP=2.86 bar for the SI case, $\lambda$= 1.0071 and IMEP= 3.75 bar for the SACI case, and $\lambda$=1.4334 and IMEP=4.25 bar for the HCCI case; 300 consecutive cycles are shown in the Figure. It can be seen that both combustion speed and cycle-to-cycle variability strongly depend on the combustion mode, which directly affects the excitation of the pressure resonant modes. Since the applicability of the method depends on the resonant modes detection, it would be affected by the combustion mode.

Figure 5 depicts the spectrogram from two individual cycles in SI (top), SACI (center) and HCCI (bottom) combustion. The selected cycles have been marked in black (solid and dashed) in the pressure traces and heat release laws in Figure 4. The frequencies with maximum excitation for a given angular position have been marked with a black line in the spectrograms. It can be seen that the resonant frequency is sufficiently excited in most of the analyzed cycles, showing a smooth trajectory from slightly above 6 kHz at 20 CAD to near 5 kHz at 80 CAD. However, the level of the excitation strongly depends on the cycle and combustion mode considered.

For the case of SI combustion, the level of excitation is significantly lower and depending on the individual cycle selected, excitation may be almost inexistent (as in the case of the example in the top-left plot). As a rule of the thumb, only slightly knocking cycles get a sufficient level of excitation when operating with SI combustion. In the case of both SACI and HCCI, combustion is very fast and resonance is clearly excited for most of the cycles.

As expected, pressure waves are damped with the gas expansion, and in some cases, as in the left cycle for SACI combustion (center) and the right cycle for SI combustion (top), excitation is not sufficient for a correct $f_{cyl}$ detection with $\alpha > 60$, which causes discontinuities in the $f_{cyl}$

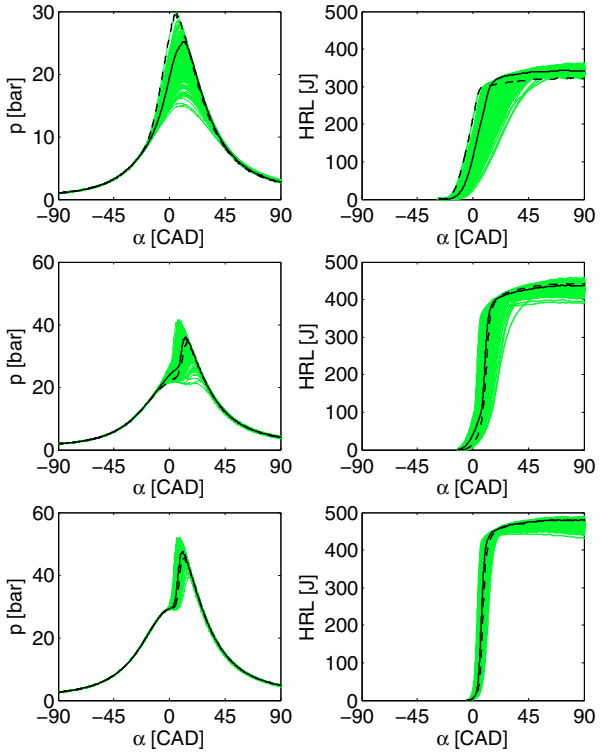


Fig. 4. Pressure traces and HRL for 300 consecutive cycles in an steady operation point with SI (top), SACI (center) and HCCI (bottom) combustion. Black lines correspond to the individual cycles analyzed in Figure 5.

trajectory estimation. Such damping of the pressure waves during the expansion stroke justify the need of limiting the range for the sliding detection window, which for this study has been set from $\alpha_0 = 35$ CAD, when combustion is finished, to $\alpha_1 = 50$ CAD, when resonance is still detectable in most of the cycles.

For the present work, the calibration of the Bessel coefficient $B\left(\alpha\right)$ was done considering that the cylinder behaves as a cylinder of infinite length when the piston is sufficiently far from the top dead center. Thus, only in-cylinder pressure information was used. Since the excitation in HCCI combustion is higher than in the rest of operating conditions, 3000 consecutive cycles of a single operation point with such combustion mode were used. The top plot in Figure 6 shows the traces of $B\left(\alpha\right)/\sqrt{m_{cyl}}$ for tl 3000 cycles. The median of the traces (solid line) and the interval defined by the standard deviation (dashed) is also shown. Outliers, marked in gray in the plot and defined as the points out of the 1-$\sigma$ interval were less than 5% of the considered samples, while 79.9% of the cycles has all samples inside the confidence region. Finally, considering that at the end of the expansion $B = 1.841$, the value of tl average $m_{cyl}$ for that operating point may be determined through (14); then the complete function $B\left(\alpha\right)$ may l computed by (13), as shown in bottom plot of Figure 6. In the latter plot, a detection window from 35 to 50 CAD has been also shown with dashed lines. Outliers for the same operation point in this range are less than 2.5%. Once the calibration for $B\left(\alpha\right)$ was obtained, it was kept constant

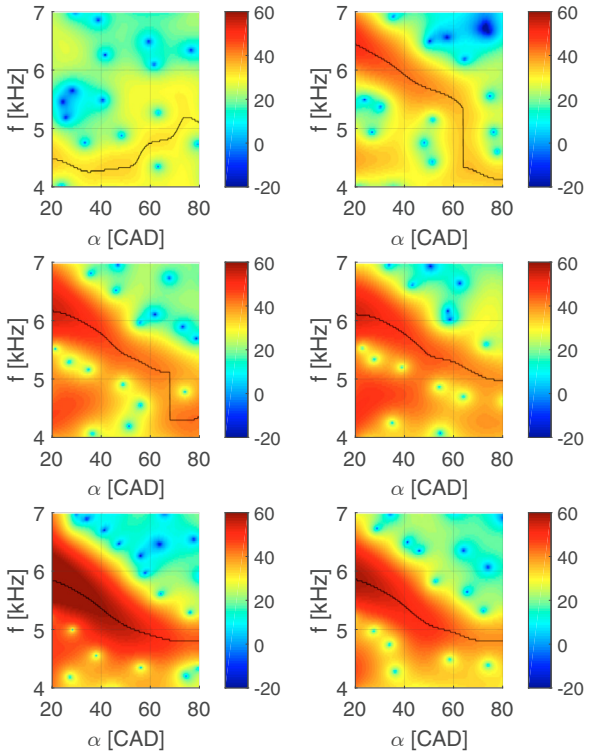


Fig. 5. Spectrogram of the in-cylinder pressure for two different cycles, for SI (top), SACI (center) and HCCI (bottom) operation; black line indicates the frequency with the maximum amplitude for a given angular position. Left plot corresponds to the dashed line in Figure 4, and right plot to the solid line. Power spectral density is expressed in logarithmic scale (dB/rad/sample).

for the rest of the work and the method was then applied to different steady operation points.

Figure 7 shows the results obtained for the operating points in Figure 4, with SI (top), SACI (center) and HCCI (bottom). For each one of the operating conditions, cycle-to-cycle results for residuals (top) and exhaust mass (bottom) are shown, as well as the median for the proposed method (solid line) and for the reference method (dashed). The proposed method results (green) for $m_{res}$ and $m_{exh}$ are compared with the Yun and Mirsky method $m_{res}$ results (gray) and the measured exhaust flow $m_{exh}$ using $m_f + m_a + m_{egr}$ values, respectively. The right side plots show the histograms of the results of the proposed method (green) and of the Yun and Mirsky method (gray). The histogram for the measured exhaust mass is not provided since the sensors where not fast enough.

It can be seen in Figure 7 that the median results of the proposed method match very well that of the reference methods in both residual and exhaust mass. However, qualitative differences may be found depending on the combustion mode considered. For the case of SI combustion (top), most of the cycles were rejected due to a value of $\sigma_{m_{cyl}} > \sigma_{thr}$. Only a fraction of the cycles (22.33% for the presented operating point and selected standard deviation threshold $\sigma_{thr}$) provided an estimate of the residual and exhaust masses. In other SI operating conditions it was not possible to apply the method since most of the cycles had

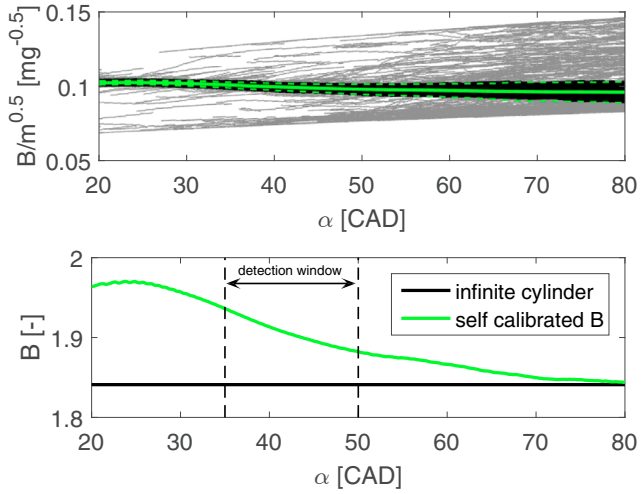


Fig. 6. Calibration of the Bessel coefficient. Top plot represents $B(\alpha)/\sqrt{m_{cyl}}$ for 3000 consecutive cycles at a given HCCI condition; median is marked as a solid line and 1-$\sigma$ interval with the dashed lines. Bottom plot uses the median from the top plot with the $m_{cyl}$ derived from (14) with $\alpha_\infty$=80 CAD, thus satisfying that the terminal value of $B$ is that of a cylinder of infinite length.

not sufficient resonance excitation. In SACI (center) and HCCI (bottom) combustion, most of the cycles yield to an estimate (82.67% and 93.67% respectively for the points shown). These results are in line with previous studies using the pressure resonance for total mass estimation on RCCI (Guardiola et al., 2014), HCCI (Luján et al., 2016) and CI (Broatch et al., 2015a) engines.

Another observation from the proposed method results is that they show a lower cyclic variability in the residual mass when compared to the Yun and Mirsky method. This could be a result of the assumption of constant cycle-to-cycle exhaust mass used in Yun and Mirsky method, which is not strictly true. In the case of the proposed method, the variability is divided between the exhaust mass $m_{exh}$ and the residual mass $m_{res}$. Part of this variation is expected to be a random noise, while the rest could be due to cycle-to-cycle variation of the quantities.

To evaluate the linearity of the proposed method, a sweep of engine operating conditions was performed under SACI combustion. Figure 8 compares the exhaust mass flow results of the proposed method with the test cell measurement (black squares) and the residual mass estimation results of the proposed method with that provided by the Yun and Mirsky method (light green circles). Error bars represent the cycle-to-cycle standard deviation. It can be seen that the method exhibits excellent linearity, where $r^2 = 0.997$ and the mean average error $MAE = 2.8$ mg/str. It must be highlighted that the calibration of the method was done without considering any mass measurement, so results could be improved by canceling any calibration bias through the fine tuning of $B$.

Lastly, the transient potential of the method was checked by performing sharp changes in cam phasing during experiments. Figure 9 shows two examples of steps in valve timing. The left plots show a step actuation in exhaust

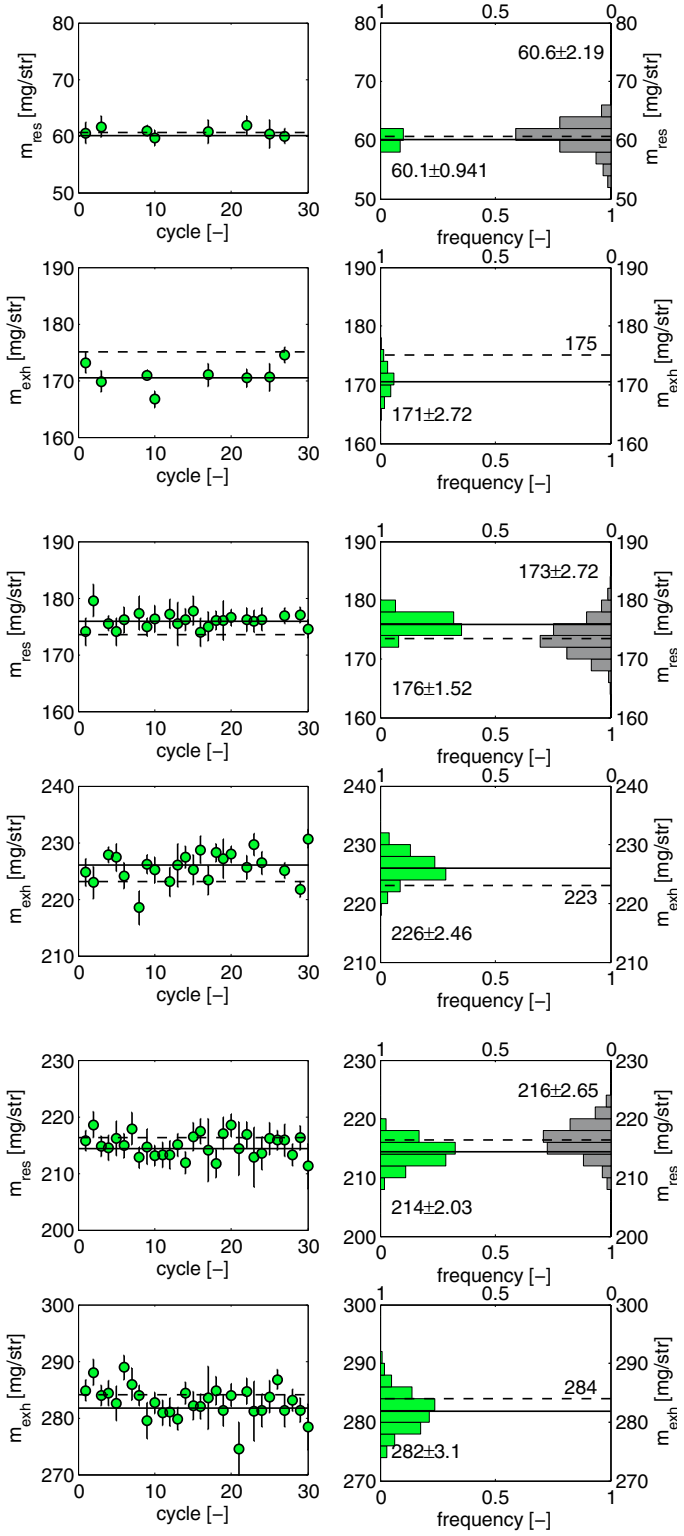


Fig. 7. Left: results over 30 consecutive cycles for a steady operation point, for SI (top), SACI (center) and HCCI (bottom) operation for both $m_{res}$ and $m_{exh}$; error bars represent intra-cycle standard deviation according to (7); solid line is median value for the method and dashed line is the mean value of the test cell (for $m_{exh}$) or Yun and Mirsky method (for $m_{res}$). Right: histograms for 300 cycles at the same operation conditions for the presented method (left) and the Yun and Mirsky method (right).

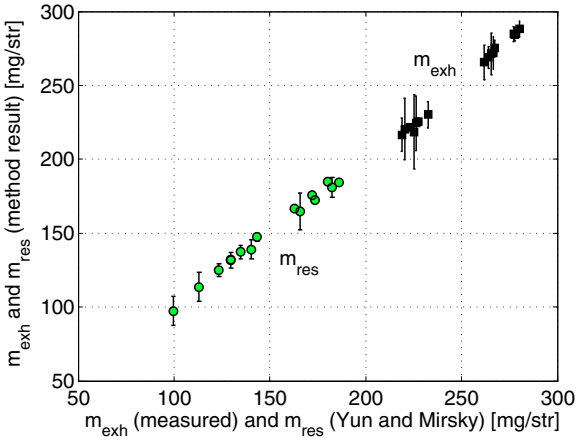


Fig. 8. Scatter plot for different operative conditions with SACI combustion, comparing $m_{exh}$ with $m_a + m_f + m_{egr}$ measurement (black squares), and $m_{res}$ with the estimation provided by Yun and Mirsky method (light green circles). All operating conditions are at 2000 rpm and nearly stoichiometric combustion, while boost pressure varies from 0.87 to 1.40 bar, IMEP from 3.5 to 4.3 bar. Error bars correspond to the cycle-to-cycle standard deviation.

cam phaser, thus providing a sharp variation in both EVO and EVC (not shown). Both EVO and EVC timing is shifted at cycle 1000, and back to the original position at cycle 2000. The central and lower plots shows the method results for the residual and the exhaust mass respectively. It can be seen that the results provided by the proposed method change between two probability distributions without significant dynamics, thus illustrating the ability of the method for transient operation. Right plots show the results of a similar transient in IVO and IVC timing, with identical conclusion.

## 5. CONCLUSIONS

The method presented in Guardiola et al. (2014) has been extended in this work to include the estimation of residuals in an NVO engine. It is based on the analysis of the in-cylinder pressure signal and does not need any flow measurement. If sufficient excitation of the resonant modes exists, the method provides a cycle-to-cycle estimation of both exhaust (and intake) mass and residual mass. It can be easily integrated in real time prototyping systems for next cycle control.

The excitation of the pressure resonance strongly depends on the type of combustion used. While in the case of SI combustion it is only possible to apply the method if some knocking occurs, SACI and HCCI combustions provide sufficient excitation in most of the cycles. The method has shown a very good linearity when compared with the test cell sensors for the mass flow though the engine, and with Yun and Mirsky method for the residual estimation. In addition, the method predicts a lower cycle-to-cycle variability of the residual mass, but considers a variability in the intake mass.

Lastly, as the proposed method provides insight into the cycle-to-cycle cylinder load and composition, it may be

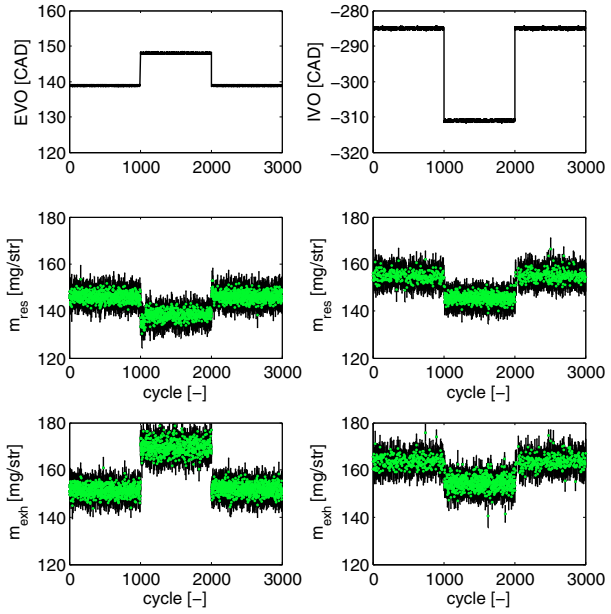


Fig. 9. Method results for a sharp actuation on exhaust (left) and intake (right) valve timing. Green dots and error bars indicate the cycle average and the intra-cycle standard deviation respectively, as in (7).

an excellent tool for analyzing the causes of combustion phasing variability.

## 6. ACKNOWLEDGEMENTS

C. Guardiola research has been partially funded by the Fulbright Commission and the Spanish Ministerio de Educación, Cultura y Deporte through grant PRX14/00274, and Spanish Ministerio de Economía y Competitividad through project TRA2013-40853-R.

## REFERENCES

Broatch, A., Guardiola, C., Bares, P., and Denia, F.D. (2015a). Determination of the resonance response in an engine cylinder with a bowl-in-piston geometry by the finite element method for inferring the trapped mass. *Int. Journal of Engine Research*, 1468087415589701.

Broatch, A., Guardiola, C., Pla, B., and Bares, P. (2015b). A direct transform for determining the trapped mass on an internal combustion engine based on the in-cylinder pressure resonance phenomenon. *Mech. Syst. Signal Process.*, 62, 480–489.

Cairns, A. and Blaxill, H. (2005). The effects of combined internal and external exhaust gas recirculation on gasoline controlled auto-ignition. *SAE Tech. Paper 2005-01-0133*.

Desantes, J.M., Galindo, J., Guardiola, C., and Dolz, V. (2010). Air mass flow estimation in turbocharged diesel engines from in-cylinder pressure measurement. *Experimental Thermal and Fluid Science*, 34(1), 37–47.

Draper, C.S. (1935). *The physical effects of detonation in a closed cylindrical chamber*. National Advisory Committee for Aeronautics.

Fitzgerald, R.P., Steeper, R., Snyder, J., Hanson, R., and Hessel, R. (2010). Determination of cycle temperatures and residual gas fraction for HCCI negative valve overlap operation. *SAE Tech. Paper 2010-01-0343*.

Guardiola, C., Pla, B., Blanco-Rodriguez, D., and Bares, P. (2014). Cycle by cycle trapped mass estimation for diagnosis and control. *SAE Int. Journal of Engines*, 7(2014-01-1702), 1523–1531.

Hellström, E., Larimore, J., Jade, S., Stefanopoulou, A.G., and Jiang, L. (2014). Reducing cyclic variability while regulating combustion phasing in a four-cylinder HCCI engine. *IEEE Trans. Control Syst. Technol.*, 22(3), 1190–1197.

Hellström, E., Stefanopoulou, A.G., and Jiang, L. (2013). Cyclic variability and dynamical instabilities in autoignition engines with high residuals. *IEEE Trans. Control Syst. Technol.*, 21(5), 1527–1536.

Hickling, R., Feldmaier, D.A., Chen, F.H., and Morel, J.S. (1983). Cavity resonances in engine combustion chambers and some applications. *The Journal of the Acoustical Society of America*, 73(4), 1170–1178.

Larimore, J., Hellström, E., Jade, S., Stefanopoulou, A., and Jiang, L. (2015). Real-time internal residual mass estimation for combustion with high cyclic variability. *Int. Journal of Engine Research*, 16(3), 474–484.

Larimore, J., Jade, S., Hellström, E., Stefanopoulou, A.G., Vanier, J., and Jiang, L. (2013). Online adaptive residual mass estimation in a multicylinder recompression HCCI engine. In *ASME 2013 Dynamic Systems and Control Conference*, V003T41A005–V003T41A005.

Lavoie, G.A., Martz, J., Wooldridge, M., and Assanis, D. (2010). A multi-mode combustion diagram for spark assisted compression ignition. *Combust. Flame*, 157(6), 1106–1110.

Luján, J.M., Guardiola, C., Pla, B., and Bares, P. (2016). Estimation of trapped mass by in-cylinder pressure resonance in HCCI engines. *Mech. Syst. Signal Process.*, 66, 862–874.

Manofsky, L., Vavra, J., Assanis, D.N., and Babajimopoulos, A. (2011). Bridging the gap between HCCI and SI: Spark-assisted compression ignition. *SAE Tech. Paper 2011-01-1179*.

Ortiz-Soto, E.A., Vavra, J., and Babajimopoulos, A. (2012). Assessment of residual mass estimation methods for cylinder pressure heat release analysis of HCCI engines with negative valve overlap. *J. Eng. Gas Turb. Power*, 134(8), 082802.

Payri, F., Galindo, J., Martín, J., and Arnau, F. (2007). A simple model for predicting the trapped mass in a DI diesel engine. *SAE Tech. Paper 2007-01-0494*.

Wheeler, J., Polovina, D., Frasinel, V., Miersch-Wiemers, O., Mond, A., Sterniak, J., and Yilmaz, H. (2013). Design of a 4-cylinder GTDI engine with part-load HCCI capability. *SAE Int. Journal of Engines*, 6(2013-01-0287), 184–196.

Woschni, G. (1967). A universally applicable equation for the instantaneous heat transfer coefficient in the internal combustion engine. *SAE Technical Paper 670931*.

Yun, H. and Mirsky, W. (1974). Schlieren-streak measurements of instantaneous exhaust gas velocities from a spark-ignition engine. *SAE Tech. Paper 741015*.

Zhao, H., Li, J., Ma, T., and Ladommatos, N. (2002). Performance and analysis of a 4-stroke multi-cylinder gasoline engine with CAI combustion. *SAE Tech. Paper 2002-01-0420*.